COMPDYN 2017
6th ECCOMAS Thematic Conference on
Computational Methods in Structural Dynamics and Earthquake Engineering
M. Papadrakakis, M. Fragiadakis (eds.)
Rhodes Island, Greece, 15–17 June, 2017

EXPERIMENTAL ASSESSMENT OF CARBON FIBER JACKETING OF STEEL PLATES

Salvatore Sessa[1], **Ferdinando Toraldo**[1],
Francesco Marmo[1], **Daniele Masi**[1] **and Luciano Rosati**[1]

[1]University of Naples Federico II
Department of Structures for Engineering and Architecture
Via Claudio 21, 80125, Napoli, Italy
e-mail: salvatore.sessa2@unina.it

Keywords: Jacket steel, Inverse identification, Fiber reinforced, Cohesive fracture

Abstract. *It is presented a numerical assessment of experimental data concerning Mode–II delamination tests of steel plates jacketed with Carbon fiber textile sheets. In particular, an inverse identification procedure, based on finite element analysis, has been performed in order to estimate the constitutive parameters of the interface bonding steel and textile. Such a procedure proved to be capable of characterizing a constitutive model which reproduces with sufficient accuracy the peak load and the fracture triggering propagation of the bonding interface. The identified finite element model is accurate enough to be employed in force–based design or in structural analysis where a suitable displacement–ultimate limit state is considered.*

The contribution analyzes the physical interpretation of the Mode–II delamination process with particular focus on its representation by means of finite element models. In particular, a discussion about the delamination process will show the consistency of the finite element model with the physical behavior of the specimen observed during the experimental tests. Such considerations, although encouraging, introduced further issues which outlines future research directions in order to improve the identification strategy.

1 INTRODUCTION

Use of Fiber–Reinforced Polymers (FRP) composites for reinforcing structural elements is a widely diffused technology particularly suitable for the structural retrofit of concrete and masonry structures. More recently, some peculiar FRP features made the scientific community explore possible applications in reinforcing steel elements [1, 2].

The fast installation of FRP devices, accompanied by the high strength–to–weight rate, results in a minor disturbance of structural functionality. Further advantages concern their mechanical properties and lay-up protocols; in particular, FRP textiles are capable of following curved or irregular surfaces of a structural element where steel plates require a preliminary grinding. In addition, the most appealing feature concerns the use of polymeric adhesives instead of welded and bolted joints [3] what allows one to avoid residual stress and steel weakening due to high temperatures [4].

The chance of using FRP in conjunction with steel elements introduces the necessity to properly account for the mechanical characterization of jacketing–substrate adhesion. In particular, the high strength of metallic adherends characterizes the interface as a well–identified region establishing a force/displacement relationship where the damage is likely to be concentrated. For this reason, it is usual to focus on *fracture* rather than adhesion. Nevertheless, these are two aspects of the same physical phenomenon: similarly to adhesion, fracture is a progressive process in which adhesion forces, acting on an extended region, contrasts the separation of two bonded interfaces.

To properly model fracture propagation several models, based on both theoretical and experimental research, have been developed. While microscale approaches [5] are capable of reproducing the interface behavior, their application in design practices is arduous; on the contrary, Cohesive–Zone Models (CZMs), originated from the original proposal by Barenblatt [6] and Dugdale [7], characterize the stress state in bonding interfaces near to crack regions.

The constitutive model of the cohesive–zone is usually defined by means of physical parameters, such as interface strength and fracture energy (thoughness), whose experimental calibration is based on testing standardized specimens. In order to characterize the constitutive parameters, several approaches are available.

A first methodology consists in the definition of theoretical models establishing closed–form relations between constitutive parameters and experimental response, as in the case of beam–theory [8, 9], compliance [10] and elasto–plastic [11] approaches.

Despite of their easy–to–use attitude, the applicability of the previous methods is conditioned to a stable propagation of the fracture during the experimental test [12]. In this sense, whenever underlying hypothesis of the theoretical model are not satisfied, the experimental test cannot define any reliable parameter.

On the contrary, recently developed inverse–identification procedures based on Finite Element (FE) analysis [13] avoid the above mentioned drawbacks. They reproduce the monitored quantities of the experimental test by means of a finite element model that adopt the quantities to be identified as parameters; an objective function measures the residual between the FEM and the experimental response [12, 14, 15]. Subsequently, numerical optimization strategies can be performed in order to identify the parameters' values that minimize the residual norm.

The significant versatility of finite elements, as well as the chance of selecting the minimization algorithm depending on the peculiar features of the experimental records [16], make inverse identification a very powerful tool.

In particular this research aims to identify the constitutive parameters of a specimen typol-

ogy consisting of steel plates reinforced with Carbon–FRP textiles, tested in a round–robin experimental campaign.

Record datasets of experimental tests, presented in Section 2, monitor the behavior of the tested specimens by means of overall load–displacement and local strain responses. Although not exhaustive of fracture propagation, the datasets are sufficiently detailed to describe the non-linear interaction between steel and FRP.

Test responses are then reproduced by a finite element model in order to define objective functions as the least–square difference between estimated and experimental responses. The FEM model is used in an optimization procedure, described in Section 3, in order to identify the parameters of the interface constitutive model.

Numerical results are discussed in Section 4 where a physical interpretation and considerations about the acceptability of the identified parameters are discussed.

Finally, conclusions provided in Section 5 discuss the open issues of the proposed strategy introducing future research directions.

2 MODEL SPECIFICATIONS AND MODE-II EXPERIMENTAL TEST

Experimental tests were carried out on symmetric specimens constituted by two $S355J0$ steel plates bonded to uniaxial Fiber reinforced textile. Steel plates, designed in order to remain elastic during the fracture tests, are cured by mechanical brushing.

The two steel plates are therefore bonded by four layers of the uniaxial Carbon–fiber textile *FiberFIP CARBON T-UNI 390*, crafted by the *FIP Chemicals S.r.l.*, applied by room–temperature impregnation with bi–component epoxy resin type *FiberFIP ADESIVO 800*, produced by the same manufacturer.

Characteristic mechanical parameters of CFRP textile and epoxy adhesive are reported in Table 1 while the adopted geometrical scheme is shown in Figure 1 where only half specimen is represented due to its symmetry. It is worth being emphasized that, although inducing flexure, the bonding is applied only on the bottom surfaces of the plates in order to detect the strain both in the CFRP and in the steel.

CFRP textile		
Parameter	Units	Value
Tensile Stress $f_{tk} = f_m - 3\delta$	MPa	≥ 2400
Avg Ult. strain	$\%$	≥ 0.6
Elastic Moduli	GPa	390
Textile Weight	g/m^2	450
Fiber Eq. thick.	mm	0.247

Epoxy adhesive		
Parameter	Units	Value
Weight Ratio $(A : B)$		$3.3 : 1$
Weight $(A + B)$	kg/dm^3	$1.10 + 0.05$
Compr. stress (23°C)	MPa	≥ 90
Flex. stress (23°C)	MPa	≥ 36
Flex.-Trac. stress	MPa	≥ 50
Adhesion to steel for direct traction	MPa	≥ 14

Table 1: Characteristic Values of Mechanical parameters of the CFRP textile and of the bi–components epoxy adhesive

A set of five symmetrically located measurement devices has been used in order to record the strain evolution during the delamination test: strain gauges of type *HBM Hottinger Baldwin Masstechnil GmbH* – $6\,mm$, *k-factor* $2.16 \pm 1.0\%$ have been applied on the external surfaces of both the steel and the CFRP, as shown in Figure 1. Specifically, strain gauges $SG1$ and $SG5$ are applied on the top surface of the steel plates simmetrically with respect to the midspan.

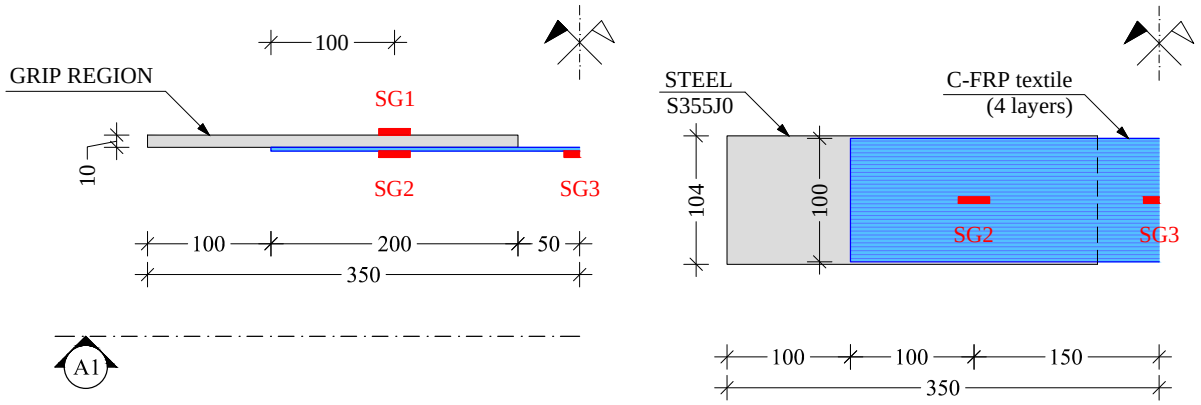

(a) Frontal view of half specimen.

(b) Plan view of half specimen.

Figure 1: Geometric layout of the tested Specimen (lengths in mm).

(a) Specimen $S1$ before the test.

(b) Specimen $S1$ after delamination.

Figure 2: Pure Mode–II delamination test $S1$.

Moreover, $SG2$ and $SG4$ have been fixed on the external surface of the CFRP textile. Gauge $SG3$, applied on the CFRP textile, is located at the middle point of the specimen and its record is inconsequential for the purposes of the present identification.

Experimental data illustrated in this contribution are referred to two Mode–II delamination tests carried out by a load–control electromechanical testing system type *MST810*, as shown in Figure 2(a). Loading, displacements and strains were recorded by the internal toolkit of the testing machine.

Both tests were carried out by monotonically increasing a quasi–static tensile load until complete delamination of the specimens, shown in Figure 2(b), was attained. Records of both experimental tests are reported in Figure 3. Specifically, load–displacement curves are plotted in Fig. 3(a) while Fig. 3(b) reports the loading plotted vs. the strain values recorded by strain–gauges $S4$ and $S5$ on the horizontal axis. It should be emphasized that both tests provided consistent experimental dataset since the differences between load–displacement curves and strains are negligible, as expected considering the natural dispersion of mechanical parameters. For

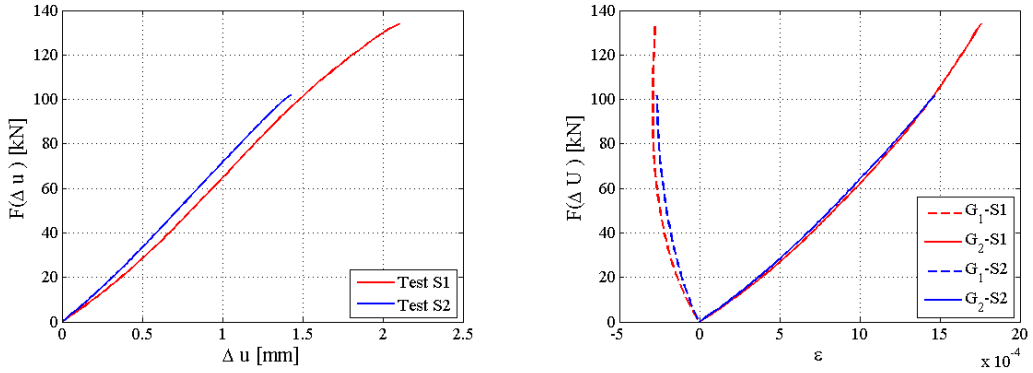

(a) Load–displacement curves. (b) Strain gauges record.

Figure 3: Mode–II delamination experimental test dataset.

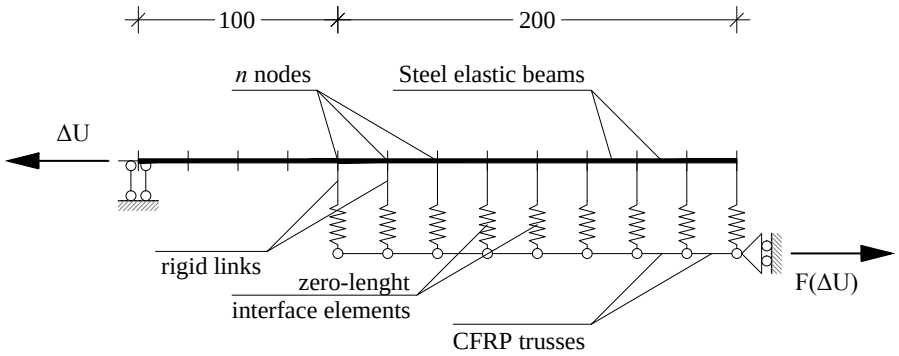

Figure 4: Scheme of the Finite Element model of the delamination test (lengths in mm).

this reason, the experimental dataset can be reasonably employed in inverse identification of adhesion constitutive parameters, an issue pursued in the following subsection.

3 INVERSE IDENTIFICATION PROCEDURE

In order to perform inverse identification of the adhesion parameters, the response of the pure Mode–II delamination test is reproduced by a Finite Element (FE) model analyzed in OpenSees [17], an object–oriented framework for structural analysis.

Figure 4 reports a simple scheme of the model which takes advantage of the specimen symmetry. Steel plates have been modeled by means of 30 elastic frames characterized by Young modulus $E_s = 210.0\,GPa$ and geometrical properties deduced from Fig. 1.

CFRP textiles have been modeled by elastic trusses with area $A_c = 0.247 \times 4 \times 104 = 102.752\,mm^2$, connected to the steel frames by rigid links with eccentricity $e = 6.5\,mm$; their Young's modulus has been experimentally characterized by preliminary tests and turn out to be $E_c = 424.0\,GPa$.

Interface between steel and CFRP is modeled by zero–lengths elements located at the end of rigid links and characterized by two independent constitutive models. Specifically, relationship between vertical forces and displacements is linearly elastic adopting the steel Young's modulus while the corresponding behavior in the horizontal direction is reported in Figure 5.

Such a constitutive model, proposed in [18], proved to be suitable for modeling Mode–II delamination and has become a consolidated standard in common practice [3]. It is characterized

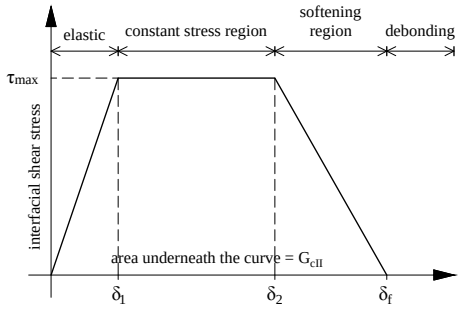

Figure 5: Typical constitutive model of the bonding interface for Mode–II delamination.

by a horizontal peak stress τ_{max} and strains δ_1, δ_2 and δ_f which have to be identified.

Fixed a trial value of the parameters, the FE estimate of the delamination test is computed that a displacement-control algorithm that applies the experimental displacements to the steel frame. In order to perform the inverse identification, it is necessary to define structural responses and an objective function Θ. In particular, for each trial value of the identifying parameters array $\boldsymbol{\beta}$, the objective function $\Theta(\boldsymbol{\beta})$ evaluates the *distance* between the FE–estimated and experimental responses.

An effective approach introduced in [14] defines $\Theta(\boldsymbol{\beta})$ as the standard deviation of the difference between recorded and estimated responses; nevertheless, it has been shown in [12] how their selection is a critical issue that can significantly influence the parameters identification.

In particular, if a structural response has low sensitivity with respect to the identifying parameters, this adds noise to the objective function what could compromise its effectiveness. In the present application, load–displacement curves shown in Fig. 3(a) present almost–linear trend with fragile collapse. This can be expected since, in case of load–control, pure Mode–II delamination presents an instantaneous propagation of the fracture. Therefore, the load–displacement relationship can characterize the initial stiffness of the system but will add very few information about the fracture propagation phase.

For this reason, an exhaustive characterization of the whole test should consider experimental records able to capture the progressive collapse of interface elements.

It has been shown in [19] that, in order to detect shear delamination, it is necessary to provide a gradual drive of the strain. For the presented tests, this progressive strain increment can be observed locally by the strain gauges. For this reason, their record has to be taken into account in the identification procedure.

In order define the objective function, the displacement governing the experimental test is discretized in m steps and is denoted as Δu_i. The experimental dataset consists of the recorded load $F^{exp}(\Delta u_i)$ and strains $\varepsilon_1^{exp}(\Delta u_i)$ and $\varepsilon_2^{exp}(\Delta u_i)$, referring to the SG1 and SG2 strain gauges, respectively.

Moreover, arranging the identifying parameters in the array $\boldsymbol{\beta} = \begin{bmatrix} \tau_{max} & \delta_1 & \delta_2 & \delta_f \end{bmatrix}$, a finite element analysis is performed adopting Δu_i as controlled displacement; it computes the parametrized responses $F^{fem}(\Delta u_i, \boldsymbol{\beta})$, $\varepsilon_1^{fem}(\Delta u_i, \boldsymbol{\beta})$ and $\varepsilon_2^{fem}(\Delta u_i, \boldsymbol{\beta})$ corresponding to the components of the experimental dataset. Denoting as R_{ld} the residual of the load and as R_{gj} with $j = 1, 2$ the residuals of the j-th strain gauge, they can be computed as:

$$R_{ld}(\Delta u_i, \boldsymbol{\beta}) = \frac{1}{m} \sum_{i=1}^{m} \left[\frac{F^{fem}(\Delta u_i, \boldsymbol{\beta}) - F^{exp}(\Delta u_i)}{F^{exp}(\Delta u_i)} \right]^2 \tag{1}$$

$$R_{gj}\left(\Delta u_i, \boldsymbol{\beta}\right) = \frac{1}{m}\sum_{i=1}^{m}\left[\frac{\varepsilon_j^{fem}\left(\Delta u_i, \boldsymbol{\beta}\right) - \varepsilon_j^{exp}\left(\Delta u_i\right)}{\varepsilon_j^{exp}\left(\Delta u_i\right)}\right]^2 \tag{2}$$

Eventually, the objective function is defined as:

$$\Theta\left(\boldsymbol{\beta}\right) = \frac{1}{3}\left[w_{ld}R_{ld}\left(\Delta u_i, \boldsymbol{\beta}\right) + w_{G1}R_{g1}\left(\Delta u_i, \boldsymbol{\beta}\right) + w_{G2}R_{g2}\left(\Delta u_i, \boldsymbol{\beta}\right)\right] \tag{3}$$

where w_{ld}, w_{G1} and w_{G2} are combination weights. Identification of the interface parameters is finally performed by the optimization problem:

$$\boldsymbol{\beta}^{\star} = \arg\min\left[\Theta\left(\boldsymbol{\beta}\right)|\boldsymbol{\beta}\right] \tag{4}$$

where $\boldsymbol{\beta}^{\star}$ is the occurrence of the parameter array which minimizes $\Theta\left(\boldsymbol{\beta}\right)$.

It is worth being emphasized that the objective function defined by Equations (1)-(3) can be physically interpreted as the mean–square of the structural response percentage residual.

4 NUMERICAL RESULTS

The procedure described in the previous section has been performed for both the introduced experimental datasets and results of the parameters identification are hereby presented.

Numerical computations have been performed by a constrained–symplex optimization algorithm available in the Matlab Optimization Toolbox v.R2013b [20] with tolerance 10^{-8}, while finite element models have been analyzed by OpenSees v. 2.2.0 [17].

Identified parameters values for both the test S1 and S2 are reported in Table 2 and corresponds to the area underneath the identified constitutive curves shown in Figure 6.

A first consideration concerns peak stress τ_{max}. In particular, let us denote as τ_{avg} the average shear stress at the specimen failure, computed as the ratio between the maximum load and the interface area and reported in the right column of Table 2. For both tests the identified values of τ_{max} are consistent with the corresponding τ_{avg}. Moreover, area underneath the constitutive curve of test S1, which is related to the Mode–II fracture energy, is consistent with the integral of experimental load displacement curve shown in Fig. 3(a). On the contrary, Test S2 presents high values of δ_2 and δ_f resulting in an over-estimation of fracture energy. For this reason, further considerations about the acceptability of the results is required.

Test	$\tau_{max}\ (MPa)$	δ_1	δ_2	δ_f	$\tau_{avg}\ (MPa)$
S1	4.1248	0.0462	0.3941	0.8421	6.4413
S2	3.6406	0.0355	1.6748	3.4138	4.8952

Table 2: Results of the parameter inverse identification

In order to qualitatively investigate if the identified parameters are significant and can be used in structural analyses, finite element responses computed at convergence have been compared with the experimental dataset.

Figures 7(a) and 8(a) present the FE and experimental load–displacement curves for the S1 and S2 test, respectively. In both cases the finite–element estimate of the load presents a good matching if initial stiffness while load at collapse turns out to be conservative with respect to the experimental curve although finite element curves present a plastic plateau.

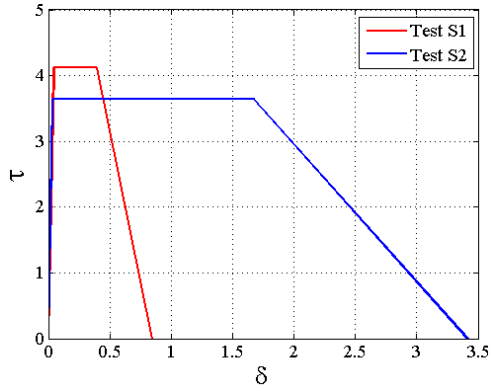

Figure 6: Identified Mode–II constitutive relationships of the interface (stress in MPa).

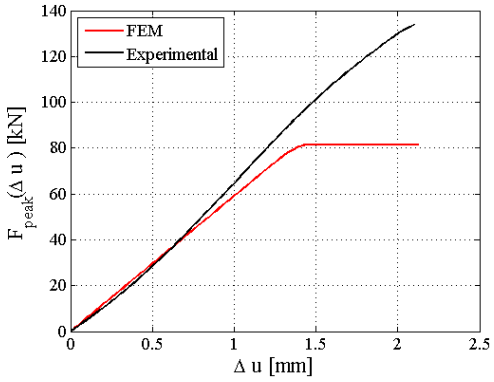

(a) Load–displacement curve.

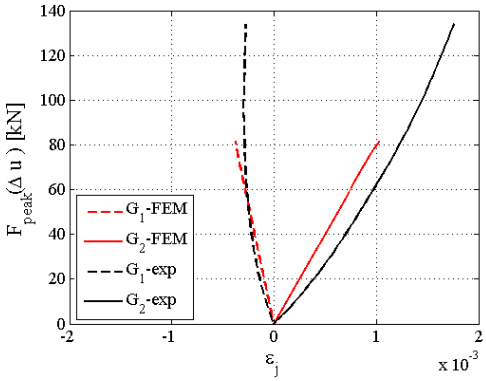

(b) Strain gauges curves.

Figure 7: Pure Mode–II delamination test $S1$. Experimental vs. identified responses.

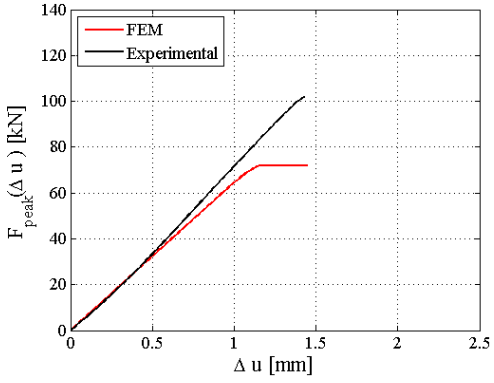

(a) Load–displacement curve.

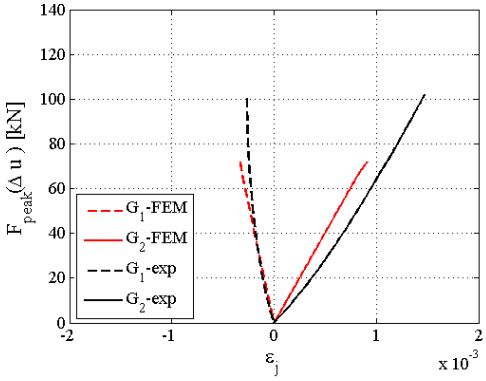

(b) Strain gauges curves.

Figure 8: Pure Mode–II delamination test $S2$. Experimental vs. identified responses.

Moreover strain responses, computed at the strain gauges application points and reported in Figures 7(b) and 8(b), show a less accurate matching with the experimental dataset, as proved by the values of the objective function computed at convergence. Recalling that the objective function Θ is defined in terms of the residual mean–square, it turns out to be $\sqrt{\Theta} = 28.11\%$ and $\sqrt{\Theta} = 23.61\%$ for test S1 and S2, respectively.

In particular such identification, obtained by adopting equal weights $w_{ld} = w_{G1} = w_{G2} = 1/3$ for all responses, is the best compromise for estimating constitutive parameters in such a way to provide acceptable matchings. Further tests with different weights, omitted for brevity, although matching the strains, fail to estimate the load.

Nevertheless, the identified parameters are capable of computing the interface responses with sufficient approximation although the plastic behavior of the load-displacement curve, as well as the over estimation of δ_2 and $ultdisp$ for test S2, require a further discussion.

Recalling the constitutive relationship reported in Figure 5, δ_1 denotes the strain value for which the fracture process is triggered while collapse of interface elements is ruled by δ_2 and δ_f. Fracture triggering and collapse do not necessarily propagate proportionally while specimens are loaded. In particular, in presence of the constitutive horizontal branch, triggering propagation is smooth since, as the interface elements reach the maximum stress, they preserve their integrity for a significant increment of strain. On the contrary, collapse propagation is expected to be fragile.

For this reason, fracture triggering results in nonlinear structural responses while collapse propagation corresponds to the sudden and complete failure of the specimen. This implies that, while nonlinearities are well recorded and can be reproduced by the finite element model, peak load represent the only information concerning the collapse. Thus, identification of τ_{max} and δ_1 is reasonably reliable while δ_2 and δ_f require further investigations.

In conclusion, the use of the identified parameters is capable to match with sufficient approximation the behavior of the bonding interface in terms of strains and maximum load while, to account for collapse, a suitable ultimate limit state should be introduced.

A final remark concerns the convergence trend of the minimization algorithm. In general, optimizations have shown good convergence as long as the parameters' starting estimates are set to physically reasonable values. On the contrary, the algorithm is not robust if its starting point does not belong to a suitable neighborhood of the solution.

This issue should be addressed by analyzing the response sensitivity with respect to the interface parameters and by defining a rule for choosing a suitable starting point of the algorithm.

5 CONCLUSIONS

Experimental and numerical assessments of Mode-II delamination tests performed on steel plates jacketed by uniaxial carbon-FRP textile sheets have been presented. In particular, the presented procedure estimates the parameters of the bonding interface constitutive model.

Experimental data have been deduced by a test protocol concerning two specimens, each one constituted by two steel plates axially jacketed by a carbon fiber textile sheet applied by means of an epoxy adhesive. The experimental dataset has been obtained driving the specimens through complete delamination and recording imposed external loads, displacements and local strains on both the steel and CFRP textile. Experimental curves present fragile collapses; nevertheless, transient nonlinear behaviors describe the propagation of the fracture triggering along the interface.

The experimental dataset has been numerically assessed in order to get the interface constitutive parameters by finite-element-based inverse identification. To this end, test responses

have been reproduced by a finite element model parameterized with respect to the identifying parameters. Subsequently, the identification procedure minimizes an objective function defined as the mean square of the difference between experimental and finite-element responses.

The values of the identified parameters proved to be capable of estimating the behavior of the bonding interface in terms of stress and strain magnitudes; moreover, the computed peak force conservatively approximates the experimental values. Nevertheless, because of the fragile failure of the tested specimens, the identified parameters are not capable of predicting the interface collapse propagation. Yet, the results can be applied in force–based structural design approaches.

Although the presented results should be considered as a preliminary stage of further investigations, they are encouraging and mark future research directions revealing some unresolved issues that should be addressed.

In particular, more refined finite element model, accounting for large displacements and local behaviors, should be used for defining the objective function and a suitable rule for fixing the starting point of the identification algorithm since this can significantly improve the accuracy of the identification. Both issues will be the topic of a future publication where constitutive behavior at collapse will be addressed by including the interface failure in the objective function.

As a final remark, some numerical results, which have been omitted for brevity, revealed a significant sensitivity of the identification procedure with respect to the constitutive parameters of the underlying (steel) adherends. Further investigations will therefore investigate such aspects by combining experimental datasets of different test typologies.

REFERENCES

[1] L. C. Hollaway, J. Cadei, *Progress in the technique of upgrading metallic structures with advanced polymer composites*, Progress in Structural Engineering and Materials 4 (2) (2002) 131–148.

[2] M. Batikha, J. Chen, J. Rotter, J. Teng, *Strengthening metallic cylindrical shells against elephant's foot buckling with FRP*, Thin-Walled Structures 47 (10) (2009) 1078 – 1091.

[3] J. Teng, T. Yu, D. Fernando, *Strengthening of steel structures with fiber-reinforced polymer composites*, Journal of Constructional Steel Research 78 (2012) 131–143.

[4] H. Jiao, X.-L. Zhao, *CFRP strengthened butt-welded very high strength (VHS) circular steel tubes* , Thin-Walled Structures 42 (7) (2004) 963 – 978.

[5] S. M. Lee, *Mode II delamination failure mechanisms of polymer matrix composites*, Journal of Materials Science 32 (5) (1997) 1287–1295.

[6] G. Barenblatt, *The Mathematical Theory of Equilibrium Cracks in Brittle Fracture*, Vol. 7 of Advances in Applied Mechanics, Elsevier, 1962, pp. 55 – 129.

[7] D. Dugdale, *Yielding of steel sheets containing slits*, Journal of the Mechanics and Physics of Solids 8 (2) (1960) 100 – 104.

[8] S. Hashemi, A. J. Kinloch, J. G. Williams, *The Analysis of Interlaminar Fracture in Uniaxial Fibre-Polymer Composites*, Proceedings of the Royal Society of London A: Mathematical, Physical and Engineering Sciences 427 (1872) (1990) 173–199.

[9] B. Blackman, J. P. Dear, A. J. Kinloch, S. Osiyemi, *The calculation of adhesive fracture energies from double-cantilever beam test specimens*, Journal of Materials Science Letters 10 (5) (1991) 253–256.

[10] J. Berry, *Some kinetic considerations of the Griffith criterion for fracture–II*, Journal of the Mechanics and Physics of Solids 8 (3) (1960) 207 – 216.

[11] M. Bocciarelli, P. Colombi, *Elasto-plastic debonding strength of tensile steel/CFRP joints*, Engineering Fracture Mechanics 85 (2012) 59–72.

[12] N. Valoroso, S. Sessa, M. Lepore, G. Cricrí, *Identification of Mode-I cohesive parameters for bonded interfaces based on DCB test* , Engineering Fracture Mechanics 104 (2013) 56 – 79.

[13] F. Ceroni, M. Ianniciello, M. Pecce, *Bond behavior of FRP carbon plates externally bonded over steel and concrete elements: Experimental outcomes and numerical investigations*, Composites Part B: Engineering 92 (2016) 434–446.

[14] R. Fedele, S. Sessa, N. Valoroso, *Image correlation–based identification of fracture parameters for structural adhesives*, Technische Mechanik 32 (2) (2012) 195 – 204.

[15] R. Sun, E. Sevillano, R. Perera, *Identification of intermediate debonding damage in FRP-strengthened RC beams based on a multi-objective updating approach and PZT sensors*, Composites Part B: Engineering 109 (2017) 248 – 258.

[16] S. Sessa, N. Valoroso, *Use of kriging to surrogate finite element models of bonded double cantilever beams*, 2015.

[17] S. Mazzoni, F. McKenna, M. H. Scott, G. L. Fenves, et al., *OpenSees command language manual*, Pacific Earthquake Engineering Research (PEER) Center.

[18] X. Lu, J. Teng, L. Ye, J. Jiang, *Bond-slip models for FRP sheets/plates bonded to concrete* , Engineering Structures 27 (6) (2005) 920 – 937.

[19] G. Cricrí, M. Perrella, S. Sessa, N. Valoroso, *A novel fixture for measuring mode III toughness of bonded assemblies* , Engineering Fracture Mechanics 138 (2015) 1 – 18.

[20] The MathWorks Inc., *Matlab R2013b user manual*, Natick, MA, USA (2013).